

**Biased Gs versus Gq and  $\beta$ -arrestin signaling in the NK1 receptor determined by interactions in the water hydrogen-bond network**

**Louise Valentin-Hansen<sup>1,2</sup>, Thomas M. Frimurer<sup>3</sup>, Jacek Mokrosinski<sup>1,2</sup>, Nicholas D. Holliday<sup>4</sup>, and Thue W. Schwartz<sup>1,2</sup>**

1. Laboratory for Molecular Pharmacology, Department of Neuroscience and Pharmacology, University of Copenhagen, The Panum Institute, Blegdamsvej 3, 2200 Copenhagen, Denmark

2. Novo Nordisk Foundation Center for Basic Metabolic Research, University of Copenhagen, Blegdamsvej 3, 2200 Copenhagen, Denmark.

3. Novo Nordisk Foundation Center for Protein Research, University of Copenhagen, Blegdamsvej 3, 2200 Copenhagen, Denmark.

4. Cell Signaling Research Group, School of Life Sciences, University of Nottingham, Queen's Medical Centre, Nottingham, NG7 2UH UK.

\*Running title: *Water hydrogen-bond network in biased receptor signaling*

To whom correspondence should be addressed: Thue W. Schwartz, Laboratory for Molecular Pharmacology, Panum Inst., University of Copenhagen, Blegdamsvej 3, Copenhagen DK-2200, Denmark. Tel.: +45-2262-2225; Fax: +45-3532-7610. E-mail: [tws@sund.ku.dk](mailto:tws@sund.ku.dk)

**Keywords:** Cell signaling, G protein-coupled receptor, receptor structure-function, molecular pharmacology, homology modeling, hydrogen-bond network, functional selectivity

**Background:** A unique Glu(2.50) in the NK1 receptor interacts directly with Ser(3.39) and Asn(7.49).

**Results:** Mutational changes in this interface create receptors which selectively signal through Gq or  $\beta$ -arrestin versus Gs.

**Conclusion:** Identification of a focal point in differentiation between Gs, Gq and  $\beta$ -arrestin signaling.

**Significance:** This network constitutes an allosteric interface essential for 7TM receptor fine-tuning towards different signaling pathways.

**ABSTRACT**

**X-ray structures, molecular dynamics simulations and mutational analysis have previously indicated that an extended water hydrogen-bond network between TM-I, -II, -III, -VI and -VII constitutes an allosteric interface essential for stabilizing different active and inactive helical constellations during 7TM receptor activation. The NK1 receptor signals efficiently through Gq, Gs and  $\beta$ -arrestin when stimulated by substance P, but lacks any sign of constitutive activity. In the water hydrogen-bond network the NK1**

**has a unique Glu residue instead of the highly conserved AspII:10 (2.50). Here we find that this GluII:10 occupies the space of a putative allosteric modulating Na<sup>+</sup> ion and makes direct inter-helical interactions in particular with SerIII:15 (3.39) and AsnVII:16 (7.49) of the NPxxY motif. Mutational changes in the interface between GluII:10 and AsnVII:16 created receptors which selectively signaled through: 1) Gq only, 2)  $\beta$ -arrestin only; and 3) Gq and  $\beta$ -arrestin but not through Gs. Interestingly, increased constitutive Gs but not Gq signaling was observed by Ala-substitution of four out of the six core polar residues of the network - in particular SerII:15. Three residues were essential for all three signaling pathways, *i.e.* the water-gating micro-switch residues TrpVI:13 (6.48) of the CWxP motif and TyrVII:20 (7.53) of the NPxxY motif plus the totally conserved AsnI:18 (1.50) stabilizing the kink in TM-VII. It is concluded that the interface between position II:10 (2.50), III:15 (3.39), and VII:16 (7.49) in the center of the water hydrogen-bond network constitutes a focal point for fine-tuning 7TM receptor conformations activating different signal transduction pathways**

Within the last decade, high resolution X-ray structures of a large number of family A seven trans-membrane (7TM)<sup>1</sup>, G protein-coupled receptors have underlined the association between highly conserved residues in the transmembrane segments and receptor function (1-4). These conserved residues are in particular located in the intracellular parts of the transmembrane helices where they function

either as micro-switches, or are involved in the large water-mediated hydrogen-bond network. This network constitutes an extended allosteric interface between the helices which perform the large-scale movements when the receptor alternates between inactive and active conformations (2,5). The water-mediated hydrogen-bond network is limited at the extracellular side by TrpVI:13 (6.48)<sup>2</sup> of the so-called CWxP motif in the middle of TM-VI, which forms the 'gate' between the network and the extracellular facing ligand-binding pocket (2). At the cytoplasmic side the network is limited by TyrVII:20 (7.53), which is part of the NPxxY motif at the intracellular end of TM-VII (Fig. 1A). Previously, by use of molecular dynamics simulations and molecular pharmacological means we have presented evidence indicating that key polar residues of this interface are essential for the signal-transduction process in the  $\beta$ 2-adrenergic receptor (B2AR) and that TrpVI:13 (6.48) and TyrVII:20 (7.53) appear to function as gates for the movements of water molecules in and out of the network (5).

The polar residues of the water hydrogen-bond network are not only highly conserved in the primary structure (Fig. 1D), but are also almost superimposable in all the other twenty unique inactive X-ray structures (Fig. 1A) solved to date (6-26). Surprisingly, the structures revealed that in the inactive state almost no hydrogen-bonds are observed between the polar residues themselves. Instead, they interact through a number of structural water molecules generating the extended hydrogen-bond network as shown for the inactive adenosine A<sub>2A</sub> receptor (A<sub>2A</sub>AR) and B2AR structures in figure 1A-C (10,16).

Interestingly, a sodium ion was identified as an important part of this network located almost identically in the A<sub>2A</sub>AR, the protease-activated receptor 1 and most recently in the 1.8 Å high-resolution structure of the δ-opioid receptor (12,26-28). In these structures, the sodium ion is coordinated by the highly conserved AspII:10 (2.50) in TM-II and SerIII:15 (3.39) in TM-III, besides nearby water molecules in a position previously shown to be taken up by either structural water molecules or left as a relatively large ‘empty space’ in X-ray structures of inactive forms of other 7TM receptors(28). Importantly, in the active structure of the B2AR and the active-like structures of the A<sub>2A</sub>AR, this region has undergone major conformational changes including the well-recognized major tilts of the intracellular parts of TM-V (inward) and TM-VI (outward) combined with an inward tilt of TM-VII (more than 2 Å combined with rotation), and an axial shift of TM-III (29,30). These movements eliminate much of the space occupied by water and the sodium ion in the inactive conformation so that in the active state the polar residues instead mainly make hydrogen-bonds directly with each other (Fig. 1C). The notion that a sodium ion stabilizes the inactive conformation of 7TM receptors, and acts as negative allosteric modulators was well-established 1½ decade ago through studies of, for example the α<sub>2a</sub> adrenergic receptor, the A<sub>2A</sub>AR, the μ- and δ-opioid receptors, and the D2 dopamine receptor (31-37). However, we now have structural proof of this interaction in the A<sub>2A</sub>AR and the δ-opioid receptor, which provides a detailed picture of how other residues besides AspII:10 (2.50) - in particular SerIII:15

(3.39) - also are involved in the binding of the allosteric negative regulator Na<sup>+</sup> (16,27,30).

In the present study we investigate the relative role of different residues in the conserved polar interface in the neurokinin-1 (NK1) receptor, which is activated by substance P and signals through both the G<sub>q</sub> and the G<sub>s</sub> pathway (38-41). A unique structural feature of the NK1 receptor is a glutamic acid residue in position II:10 (2.50), in contrast to aspartic acid found in more than 98% of other family A receptors (42). Interestingly, the unstimulated NK1 receptor is very ‘silent’ with no evidence of constitutive activity resulting from spontaneous transition to the active state. For more than two decades we have performed structure-functional studies on the NK1 receptor and have never observed measurable constitutive activity and in contrast to most other 7TM receptors, we have never identified an NK1 mutant showing ligand-independent signaling (38,43-47). This is particularly surprising as it is generally known in the field that it is rather easy to find mutations in 7TM receptors which make them signal with high constitutive activity.

We now find that in molecular models of the NK1 receptor the gamma-carboxylic acid group of the larger GluII:10 (2.50) side-chain (compared to Asp) is located at or very close to the position where the negative allosteric modulating sodium ion is found in for example the A<sub>2A</sub>AR, the δ-opioid receptor and the β<sub>1</sub>-adrenergic receptor (27,28,32,48) and that it makes direct hydrogen-bonds to other members of the water-hydrogen-bond network, SerIII:15 (3.39) and AsnVII:16 (7.49). Mutational analysis indicates that GluII:10 and its two hydrogen-

bond partners in different ways are involved in tuning Gs versus Gq and  $\beta$ -arrestin signaling and that negative modulatory  $\text{Na}^+$  effects could be induced in the NK1 receptor by ‘reintroducing’ Asp in position II:10.

### Experimental procedures

**Comparative homology modelling** - The sequence of the human NK1 receptor was obtained at the Uniprot webpage. The distinct X-ray structures (available at the time the modeling were conducted) of 7TM receptors in inactive like states: adenosine  $A_{2A}$  (4EIY),  $\beta$ 1-adrenergic receptor (2VT4),  $\beta$ 2-adrenergic receptor (2RH1), chemokine CXCR4 (3ODU), chemokine CCR5 (4MBS), dopamine D3 (3PBL), Histamine H1 (3RZE), Muscarinic M2 (3OUN) Muscarinic M3 (4DAJ), Serotonin  $5HT_{1B}$  (4IAR), Serotonin  $5HT_{2B}$  (4IB4),  $\mu$ -opioid (4DKL)  $\delta$ -opioid (4EJ4), k-opioid (4DJH), Nociceptin (4EA3), protease-activated receptor 1 (3VW7), Sphingosine S1P (3V2Y) and rhodopsin (1GZM) as well as the structures in active like states: adenosine  $A_{2A}$  (3QAK),  $\beta$ 2-adrenergic receptor (3SN6), Muscarinic M2 (4MQS), Neurotensin 1 receptor (4GRV) were obtained from the PDB database. The structures were superimposed with respect to the intracellular half of TM-I, -II, -III and -VII using the CEAlign protocol in Pymol. Pairwise sequence alignments and comparative homology models (excluding intra- and extracellular loops) of the NK1 receptor were produced in ICM 3.7b using the in-active and active like structures of  $A_{2A}$ AR and B2AR as templates which devised reasonable high sequence identity to the intracellular half of TM-I, -II, -III and -VII.

GluII:10 was assumed to be negatively charged as it is located in-between SerIII:15 and ThrVII:13 in an optimal position to be involved in hydrogen-bond interactions the hydroxyl side-chain of SerIII:15 and the co-existence of “conserved” bulky water molecules observed in other receptors with similar environments. Initially, hydrogen atoms and side-chains were optimized using the comparative modeling protocol in ICM. When modeling the inactive state of NK1R, the sodium ion and structural water molecules of the template structures were “copied” to the comparative NK1 receptor models. The location of the sodium ion and water molecules was initially accessed in the presence of a fixed NK1 receptor model. The sodium ion and a nearby water molecule, which are involved in hydrogen bond interaction with AspII:10 and SerIII:15 in the parent  $A_{2A}$ AR and B2AR structures were removed from the NK1 receptor models as they make steric clashes with the larger (compared to Asp) carboxyl acid side-chain of GluII:10 in the NK1 receptor models. Local optimization of side-chains within 8 Å of this co-localized sodium ion/water molecule was unable to release the strain when optimizing all atoms using the biased probability Monte Carlo optimization protocol (200 global moves and 100 local minimization calls). To ensure acceptance of the remaining water molecules, side-chains and water molecules were globally optimized using the Monte Carlo conformational sampling procedure in the presence of a fixed main chain conformation in ICM 3.7b. Finally, the resulting NK1 models were minimized in 300 steps of steepest decent, using the MMFF force field and all atoms were free to move. In

the present work we only present the NK1 receptor model based on A<sub>2A</sub>AR as the corresponding NK1 receptor model based on B2AR are highly similar.

**Materials-** Substance P and ghrelin were purchased from Bachem and [<sup>125</sup>I]Lys<sup>3</sup>-SP from Perkin Elmer. Pindolol was purchased from Sigma and AR-231453 was a generous gift from Arena Pharmaceuticals (San Diego, USA)

**Molecular Biology-** The NK1, B2AR and GHSR cDNA was cloned into the eukaryotic expression vector pCMV-Tag (2B) (Stratagene) while GPR119 cDNA was cloned into the pcDNA3.1 vector (Invitrogen). Mutations were constructed by PCR using the Quick Change method. All PCR experiments were performed using *Pfu* polymerase (Stratagene) according to the instructions of the manufacturer. All mutations were verified by DNA sequence analysis by MWG (Ebersberg, Germany). For  $\beta$ -arrestin recruitment cDNAs encoding native and mutant NK1 receptors were tagged at the C terminal with an enzyme donor fragment of  $\beta$ -galactosidase.

**Transfections and Tissue Culture-**COS-7 cells were grown in Dulbecco's modified Eagle's medium 1885 supplemented with 10% fetal calf serum, 2mM glutamine, 100U/ml Penicillin and 100 $\mu$ g/ml streptomycin. Cells were transfected with 20 $\mu$ g/75cm<sup>2</sup> of DNA using the calcium phosphate precipitation method with chloroquine addition as previously described (45).

CHO-K1 cells stably expressing  $\beta$ -arrestin2 tagged with the enzyme accepting portion of an  $\beta$ -galactosidase enzyme were grown in HAMF12 media supplemented with 10% fetal calf serum, 2mM glutamine, 100U/ml Penicillin,

100 $\mu$ g/ml Streptomycin and 300 $\mu$ g/ml of Hygromycin. Cells were transfected using 0.15 $\mu$ l fuGENE (Promega,WI,USA)/well in opaque white 96-well plates using 50ng DNA/well according to the manufacturer's protocol.

**Cell surface expression (ELISA)-**Cells transfected and seeded for IP<sub>3</sub> or cAMP were in parallel seeded for ELISA. The cells were washed twice with 200 $\mu$ l phosphate buffered saline (PBS), fixed with 150 $\mu$ l paraformaldehyde for 10 min and finally incubated in blocking solution (PBS plus 3% dry milk) for 30 min at room temperature. Subsequently the cells were incubated 1 hour at room temperature with anti-FLAG (M2) (Sigma) antibody diluted 1:1000. The cells were washed 3 times with PBS and incubated 1 hour at room temperature with anti-mouse horseradish peroxidase conjugated antibody (Sigma) diluted 1:1250. After 3 additional washing steps with PBS immunoreactivity were discovered by addition of horseradish peroxidase. The absorbance was read on the Topcount (Perkin Elmer).

**Competition Binding Assay –** Transfected COS-7 cells were plated in poly-D-lysine coated 96-well plates at a density of 500-20,000 cells/ well aiming at 5-10% binding of the radioactive ligand. The following day the binding experiments were performed for 3 hours at 4°C using ~25pM 125I-SP (Perkin Elmer). Binding assays were performed in 0.1ml of a HEPES buffer, pH 7.4, supplemented with 1mM CaCl<sub>2</sub>, 5mM MgCl<sub>2</sub>, 0.1% (w/v) bovine serum albumin and 40 $\mu$ g/ml bacitracin with or without increasing concentrations of NaCl. Nonspecific



binding was determined as the binding in the presence of 1 $\mu$ M unlabelled SP. After two washes in cold buffer, Lysis buffer (1% SDS, 200mM NaOH) was added for 30 min and radioactivity was counted.

**Phosphatidylinositol Turnover Assay**—One day after transfection, COS-7 cells were incubated for 24 h with 5 $\mu$ Ci of [3H]myo-inositol (catalog number PT6–271, Amersham Biosciences) in 300 $\mu$ l of medium supplemented with 10% fetal calf serum, 2mM glutamine, 100U/ml Penicillin and 100 $\mu$ g/ml streptomycin per well. Cells were washed twice in 20mM HEPES buffer (pH 7.4, supplemented with 140mM NaCl, 5mM KCl, 1mM MgSO<sub>4</sub>, 1mM CaCl<sub>2</sub>, 10mM glucose, 0.05% (w/v) fetal bovine serum), and following incubated in 0.2ml of HEPES buffer supplemented with 10mM LiCl at 37 °C for 15 min. After stimulation with SP for 45min at 37 °C, cells were extracted with 10mM formic acid followed by incubation on ice for 30 min. The resulting supernatant was purified on Bio-Rad AG 1-X8 anion exchange resin to isolate the negatively charged inositol phosphates. After application of the cell extract to the column, the columns were washed twice with GPI buffer (60mM sodium formate and 100mM formic acid) to remove glycerophosphoinositol. Inositol phosphates were eluted by the addition of elution buffer (1mM ammonium formate, 100mM formic acid). Determinations were made in duplicates. The columns containing AG 1-X8 anion exchange resin were regenerated by the addition of 3ml of regeneration buffer (3M ammonium formate, 100mM formic acid) and 10ml of water.

**cAMP Assay**—One day after transfection COS-7 cells were plated into white 96-well plates (20,000 cells/well). The day after, cAMP assay was performed using DiscoverX HitHunter™ cAMPxs+ kit (Fremont, CA, USA) according to the manufacturer's protocol.

**$\beta$ -Arrestin2 recruitment**—The day after transfection  $\beta$ -Arrestin2 recruitment was determined using DiscoverX PathHunter<sup>R</sup>  $\beta$ -Arrestin GPCR Assay (Fremont, CA, USA) according to the manufacturers protocol.

**Calculations**— $EC_{50}$  values were determined by nonlinear regression using the Prism 6.0 software (GraphPad Software, San Diego). Unpaired t-test ( $P < 0.05$ ) was performed using the Prism 6.0 software (GraphPad Software, San Diego).

## Results

### *Modeling of the polar network in the NK1 receptor*

Analysis of 20 unique inactive 7TM receptor structures in complexes with inverse agonists or antagonists demonstrated that polar, water- and sodium ion-coordinating residues of the conserved interface between the intracellular segments of TM-I, -II, -III and -VII, can be almost perfectly superimposed (Fig. 1A and 1B) (7,8,10-21,23-26,49,50). This is in contrast to residues in the extracellular ligand-binding pocket, which shows larger variations in sequence and structure. Although a sodium ion has only been directly identified in this polar interface of the A<sub>2A</sub>AR, protease-activated receptor 1 and the  $\delta$ -opioid receptors, there is also clearly room for it, in between the highly conserved AspII:10 (2.50) and SerIII:15 (3.39),

in all other inactive receptor conformations (37). In contrast, in the molecular model of the inactive conformation of the NK1 receptor, the gamma carboxyl side-chain of GluII:10 replaces the sodium ion and/or one or more water molecules making direct rather than water-mediated interactions with not only SerIII:15 (3.39) but also with AsnVII:16 (7.49) (Fig. 1E,1F and Fig. 2A). The helix organization and side-chain packing of the energy optimized NK1 receptor models are highly similar to the inactive experimental structures when superimposed with respect to conserved key residues in the intracellular half of TM-I, -II, -III and -VII. Either of the water molecules in the refined models deviate more than 0.75 Å from their original positions and rotamer states of side-chains involved in the water mediated hydrogen bonds remain unchanged. In addition, GluII:10 (2.50) interacts with TyrVII:20 (7.53) through hydrogen-bond interactions with a single water molecule, in contrast to the interaction of AspII:10 (2.50) with TyrVII:20 (7.53) in the inactive structures of A<sub>2A</sub>AR and B2AR, which is mediated through two water molecules (5,10,51).

In the models of the active conformation of the NK1 receptor built over the active structures of the B2AR-Gs and A<sub>2A</sub>AR receptors (16,29) the volume of the polar interface is greatly reduced due to the inward movement of TMVII toward TMIII by more than 2Å, which effectively ‘squeezes’ out the possible sodium ion and most of the structural water molecules (Fig. 2A and 2B). In this model, the carboxylic acid side-chain of GluII:10 (2.50) could either be making direct interactions with SerII:15 (3.39),

ThrVII:13 (7.46) and AsnVII:16 (7.49) or direct interactions with SerIII:15 (3.39) and AsnVII:16 (7.49) depending on the detailed side-chain packing (Fig. 2B).

In conclusion, the gamma carboxyl side-chain of GluII:10 (2.50) in the NK1 receptor appears to be substituting the Na<sup>+</sup> in the polar interface making direct instead of water-mediated hydrogen-bond interactions to other members of the hydrogen-bond network (Fig. 2b).

#### ***Functional effects of Ala-substitution of the polar residues in the NK1 hydrogen-bond network***

The functional importance of each residue in the water hydrogen-bond network of the NK1 receptor was probed by Ala-substitutions and constitutive and SP-induced signaling were determined for the three different signal transduction pathways: 1) Gq signaling monitored by IP<sub>3</sub> accumulation assay (Fig. 3); 2) Gs signaling monitoring by cAMP production (Fig. 4); and 3) β-arrestin mobilization measured by an enzyme complementation assay (Fig. 5). The effect of the mutations on cell surface expression was determined for each of the mutants using cell surface ELISA (inserts in Fig. 3).

#### ***Effects of Ala-substitutions on Gq signaling***

Ala-substitution of each of the two micro-switch residues TrpVI:13 (6.48) of the CW<sub>x</sub>P motif in TM-VI and TyrVII:20 (7.53) of the NP<sub>x</sub>xY motif in TM-VII, which place respective extracellular and intracellular limit on the hydrogen-bond network eliminated SP-induced signalling of the NK1 receptor through the Gq pathway as determined by IP<sub>3</sub> accumulation (Fig. 3h, i and table I). Ala-substitution of the

almost 100% conserved AsnI:18 (1.50), which in the inactive receptor structures form a direct hydrogen bond to the backbone carbonyl group of ThrVII:13 (7.46) that is exposed at the helical kink in TM-VII (2), also eliminated SP-induced Gq signalling (Fig. 3d). Similarly, Ala-substitution of GluII:10 (2.50) totally eliminated SP-induced Gq signalling (Fig. 3c). There was no indication of increased constitutive Gq signalling in the GluII:10 to Ala mutant receptor (Fig. 3c), which otherwise could have been expected based on the potential function of GluII:10 as a tethered negative allosteric regulator as discussed in the molecular modelling section above. In TM-VII, Ala-substitution of SerVII:12 (7.45) impaired the SP-induced IP<sub>3</sub> accumulation down to 35% of the E<sub>max</sub> observed in the wild-type receptor (Fig. 3f, table I). In contrast, Ala-substitution of AsnVII:16 (7.49) one helical turn below, which we previously found to be essential for Gs signalling in the B2AR, had surprisingly almost no effect on the SP-induced signalling through the Gq pathway in the NK1 receptor (Fig. 3g). Similarly, Ala-substitution of ThrVII:13 (7.46) and SerIII:15 (3.39) in TM-III located at the top of the water hydrogen-bond network had no or very little effect on the Gq signalling in the NK1 receptor (Fig. 3b,e).

#### ***Effects of Ala-substitutions on Gs signaling***

As observed for Gq signaling, Ala-substitution of the two water-gating micro-switch residues TrpVI:13 (6.48) and TyrVII:20 (7.53) as well as Ala-substitution of AsnI:18 (1.50) and GluII:10 (2.50) eliminated Gs signalling through the NK1 receptor as measured by SP-induced cAMP accumulation and showed no sign of constitutive

Gs signalling either (Fig. 4h,i,d,c). In contrast, increased basal cAMP production in the absence of agonist was observed not only in GluII:10 but in all of the Ala mutations of the conserved polar residues, except for the mutant forms of SerVII:12 (7.45) and AsnVII:16 (7.49) (Fig. 4, Table I). In particular the SerIII:15 (3.39) to Ala mutant showed a highly increased constitutive Gs signalling of 37+/-6% of E<sub>max</sub> of the wild type receptor corresponding to 24% of its own somewhat increased E<sub>max</sub> (Fig. 4). In case of the AsnI:18 and GluII:10 substitutions the SP-induced cAMP response was totally eliminated despite the slightly but significant increased basal Gs signalling of the AsnI:18 and GluII:10 mutants. Surprisingly in view of the lack of effect on Gq signaling, removal of the polar side-chain of AsnVII:16 (7.49) by Ala-substitution totally eliminated Gs signalling (Fig. 3g and 4g), just as we had observed for Ala-substitution of this residue in the B2AR (5). Furthermore, the AsnVII:16 to Ala substitution did not increase basal Gs signalling (Fig. 4).

#### ***Effect of Ala-substitutions on $\beta$ -Arrestin mobilization***

As shown in Fig. 5, the effects of Ala-substitution of the residues in the water hydrogen-bond network upon  $\beta$ -arrestin mobilization were rather similar to the effects observed in Gq signaling (Fig. 3). Thus, as observed in the IP<sub>3</sub> assay, Ala-substitution of TrpVI:13 (6.48), TyrVII:20 (7.53) and AsnI:18 (1.50) in all cases eliminated SP-induced  $\beta$ -arrestin mobilization and Ala-substitution of ThrVII:13 (7.46) and SerIII:15 (3.39) located at the top of the hydrogen-bond network had almost no effect or induced a slight increase in



$\beta$ -arrestin mobilization. As for  $IP_3$  accumulation assays, a partial inhibition of the  $\beta$ -arrestin response was observed following SerVII:12 (7.46) to Ala mutation (Fig. 5f). In the AsnVII:16 (7.49) to Ala mutant, which selectively inhibited Gs but not Gq, the  $\beta$ -arrestin response almost similar to the wild-type NK1 receptor was observed (Fig. 5g). Interestingly, in the case of GluII:10 (2.50), which was totally unresponsive in both Gq and Gs signalling, SP responses were evident from  $\beta$ -arrestin mobilization, albeit only approx. 25% of the response observed in the wild type NK1 receptor (Fig. 5C).

#### ***Effect of substituting GluII:10 with Gln on NK1 signaling***

In order to examine the effect of removing the potential negative charge of GluII:10 while retaining the ability to participate in hydrogen bond formation we introduced Gln at this position. Cell surface expression of the Gln mutant was comparable to WT receptor as shown in Table I. Through the Gs pathway the Gln substitution of GluII:10 resulted in a very high constitutive signaling corresponding to almost 40% of  $E_{max}$  of the WT receptor, *i.e.* similar to what was observed with the SerIII:15 to Ala mutant (Table I). The high constitutive Gs signaling could not be further increased by the agonist SP in the GluII:10 to Gln mutant (Table I). In respect of Gq signaling, sub-nanomolar potency of SP was retained but the  $E_{max}$  was reduced to 40% of WT receptor (Table I) and in respect of  $\beta$ -arrestin mobilization a ten-fold reduction in potency of SP was observed while the max. signaling efficacy resembled WT receptor (Table I).

It is concluded that GluII:10 very likely in its charged form acts as a negative regulator of in particular Gs signaling as substitution with Gln results in very high constitutive signaling.

#### ***Effect of ‘reintroduction’ of Asp for GluII:10 on NK1 signaling and $Na^+$ modulation***

Mutating GluII:10 (2.50) into aspartic acid, as found in the vast majority of 7TM receptors, increased cell surface expression by approx. 50% as compared to wild type receptor (insert in Fig. 6a). In contrast to the Ala-substitution, the AspII:10 mutant signaled as wild type NK1 through Gq as determined by  $IP_3$ -accumulation (Fig. 6a). However, in respect of Gs signaling the AspII:10 mutant, in contrast to the Ala-substitution displayed no significant constitutive activity in the cAMP assay and had a seriously impaired SP-induced cAMP response with a reduction in potency of at least two orders of magnitude and not reaching an  $E_{max}$  with the highest concentration tested (Fig.6B). In contrast to the GluII:10 to Ala mutant, which did show a clear but diminished  $\beta$ -arrestin response to SP, the GluII:10Asp mutant did not recruit  $\beta$ -arrestin at all upon stimulation with SP (Fig. 6c).

The most clear allosteric modulatory effect of  $Na^+$  in receptors with an Asp in position II:10 is on ligand binding affinity as recently reported for the  $\delta$ -opioid receptor (27). In the wild type NK1 receptor no effect of  $Na^+$  on SP binding was observed in whole cell competition binding using radiolabeled SP in transfected COS-7 cells (Table II). However, when Asp was ‘reintroduced instead of Glu in position II:10, 300mM  $Na^+$  impaired the SP affinity from 0.11  $\pm$  0.05 nM in its absence to 1.2  $\pm$  0.5 nM in its presence (Table II), *i.e.* a negative modulating

effect similar to what has been reported for the  $\delta$ -opioid receptor (27). Ala-substitution of SerIII:15 (3.39) another residue potentially involved in coordinating  $\text{Na}^+$  in the water hydrogen-bond network, had no effect on the binding of SP in the NK1 receptor and also here no effect on  $\text{Na}^+$  was observed (Table II).

#### ***Effect of introducing Glu at position II:10 in GPR119, B2AR and the Ghrelin receptor***

The B2AR, GPR119 and the Ghrelin receptors were chosen because they display variable degrees of constitutive activity and all carry an Asp in position II:10. Introduction of a Glu residue at this position as in the NK1 receptor decreased the cell surface expression of all three receptors although they were still expressed at more than 50% of the corresponding WT receptors (Table III). In the case of GPR119 the effect of the mutation was difficult to interpret as both the constitutive activity and the  $E_{\text{max}}$  were reduced to approx. 50% of WT, *i.e.* corresponding to the reduction in expression level. However, the potency of the agonist AR231453 was also reduced, *i.e.*  $EC_{50}$  increased from 2.2 to 17 nM (Table III). In the case of B2AR, introduction of Glu at position II:10 reduced the  $E_{\text{max}}$  to 17% of WT and the constitutive activity from 9.9 to 2 % (Table III). However, the negative effect on signal transduction was most clearly observed in the ghrelin receptor, where substitution of AspII:10 with Glu totally eliminated both the constitutive signaling and the ghrelin-induced signaling (Table III).

#### **Discussion**

In the present study we tested the unique role of GluII:10 (2.50) of the water hydrogen-bond network in the NK1 receptor. Molecular modeling suggests that the side chain of GluII:10 located at a position where almost all other Family A GPCRs have an Asp residue, replaces one or more water molecules, normally found in the inactive conformations of other receptors, mediating interactions between the conserved polar residues. Consequently GluII:10 makes direct hydrogen-bond interactions to SerIII:15 (3.39) in TM-III and AsnVII:16 (7.49) of the NPxxY motif in TM-VII and thereby conceivably mimics movable water molecules and/or a putative allosteric modulating  $\text{Na}^+$  ion. As previously observed in the B2AR (5), we here find that the water-gating residues of the hydrogen-bond network are essential for signal transduction whereas GluII:10 and its interaction partners are important for fine-tuning the signaling through Gs versus Gq and  $\beta$ -arrestin (Fig. 7).

#### ***Is GluII:10 a tethered negative allosteric regulator in the NK1 receptor?***

The initial hypothesis was that GluII:10 (2.50), by replacing the  $\text{Na}^+$  ion, would function as a tethered negative allosteric modulator and account for the unusual lack of constitutive signaling by the NK1 receptor. The very high, maximal constitutive signaling through Gs observed when GluII:10 was substituted with Gln, supports this notion (Table I). These data also indicate that it is the deprotonated, charged form of the  $\gamma$ -carboxylic acid group of GluII:10 that acts as an allosteric negative modulator in the NK1 receptor in particular of Gs signaling as introduction of Gln, which has the same size and

similar hydrogen-bond potential as Glu, increased the constitutive signaling.

Surprisingly, however we only observed marginal constitutive activity through G<sub>s</sub> and no constitutive signaling through G<sub>q</sub> when GluII:10 was substituted with Ala (Fig. 3 and 4). One explanation could be that GluII:10 not only functions as an allosteric negative regulator (stabilizing an inactive conformation) but also is essential for not only the SP-induced G<sub>q</sub> signaling, as it clearly is (Fig. 3), but also is essential for the ligand-independent, constitutive signaling. In other words GluII:10 is also involved in stabilizing active conformations of the receptor, where it can be replaced by for example Gln, but not by Ala. In that case we would not be able to observe any high constitutive signaling in the Ala substituted receptor because the general importance of GluII:10 for receptor signaling would prevent that. Interestingly, although G-protein signaling was eliminated SP-induced arrestin signaling was still observed in the GluII:10 to Ala mutant. The notion that a Glu residue at position II:10 (2.50) can act as an allosteric negative regulator of receptor signaling was further supported by the deleterious effects observed when Glu was introduced instead of AspII:10 in the B2AR, GPR119 and in particular in the ghrelin receptor, where signaling was essentially eliminated. The cell surface expression was somewhat decreased in the AspII:10 to Glu mutant form of the ghrelin receptor however, we have previously studied a number of ghrelin receptor mutants having similar or even lower expression levels, who nevertheless all signaled efficiently (See Table II in (52)).

### ***Differential G<sub>s</sub> versus G<sub>q</sub> signaling through the water hydrogen-bond network***

Although most 7TM receptors are known to signal mainly through one G protein pathway they quite often are able to activate several G proteins (53-55). The NK1 receptor, for example, is best known as a G<sub>q</sub> coupled receptor activating IP<sub>3</sub> and mobilizing calcium. However, substance P in fact activates both G<sub>s</sub> and G<sub>q</sub> pathways efficiently with similar nanomolar potency (38). Interestingly, the mutational substitutions of the water hydrogen-bond network of the NK1 receptor in several aspects affected G<sub>q</sub> and G<sub>s</sub> signaling differently. Thus removal of the polar side-chain of four out of the six residues of the water hydrogen-bond network individually increased the constitutive, ligand-independent G<sub>s</sub> signaling without affecting the corresponding basal G<sub>q</sub> signaling (Fig. 4). Previously, we have observed a similar phenomenon in the B2AR, where Ala-substitution of AsnI:18, AspII:10 and SerVII:13 which jointly are coordinating the mobile water molecules in this receptor also increased the basal, ligand-independent G<sub>s</sub> signaling (5).

The agonist-induced G<sub>s</sub> versus G<sub>q</sub> signaling was also differentially affected by mutational substitutions of the hydrogen-bond network. Most notably, Ala-substitution of AsnVII:16 (7.49) of the NPxxY motif selectively eliminated G<sub>s</sub> signaling with no effect on the G<sub>q</sub> pathway. The SerVII:12 (7.45) to Ala mutant located one helical turn above in TM-VII had a similar phenotype but with a somewhat impaired G<sub>q</sub> response (Fig. 3, 4). Similarly, in the B2AR Ala-substitution of the corresponding two residues both abolished agonist-induced receptor

activation through  $G_s$  (5). Interestingly, molecular modeling studies of the  $G_s$  coupled TSH receptor suggested that AsnVII:16 (7.49) acted as an on/off switch in receptor activation, which was confirmed in functional studies as the AsnVII:16 to Ala mutant form could not be activated by TSH although it bound the agonist with wild-type affinity and displayed a normal, high constitutive basal  $G_s$  signaling (56). In the CCK receptor, the AsnVII:16 (7.49) residue has been demonstrated to be essential for  $G_q$  signaling (57). Apparently the interface between TM-II, TM-III, and TM-VII is particular important for  $G_s$  versus  $G_q$  signaling. Previously, we identified another residue located at this interface but more towards the extracellular side between TM-II and TM-III, *i.e.* PheIII:07 (3.31) which upon substitution to Ser also selectively uncoupled the NK1 receptor from the  $G_s$  pathway while leaving  $G_q$  signaling intact (38).

#### ***$\beta$ -Arrestin versus G protein signaling through the water hydrogen-bond network***

Both ligands and mutations have been shown to be able to stabilize distinct conformations leading to biased receptor signaling within specific GPCRs (4,38,58-62). As shown in Fig. 7, we here find that mutations of GluII:10 and AsnVII:16, which according to the molecular modeling in the NK1 receptor are interacting directly with each other, result in biased signaling, *i.e.* where the three signaling pathways  $G_s$ ,  $G_q$  and  $\beta$ -arrestin mobilization are differentially affected. Thus, in the AsnVII:16 to Ala mutant the  $G_s$  signaling was selectively eliminated while both  $G_q$  signaling and  $\beta$ -arrestin mobilization were similar to wild type

NK1. In contrast, in the GluII:10 (2.50) to Ala mutant both SP-induced  $G_q$  and  $G_s$  signaling were totally eliminated while the SP-induced recruitment of  $\beta$ -arrestin was rather well preserved in particular when taking into account the somewhat reduced cell surface expression (Fig. 5). Thus, removal of the acidic side-chain of GluII:10 by Ala-substitution converted the NK1 receptor into a clean  $\beta$ -arrestin-biased receptor. However, when GluII:10 instead was substituted with the shorter acidic Asp residue - as found in most other receptors -  $\beta$ -arrestin mobilization was totally eliminated and  $G_s$  signaling seriously impaired while  $G_q$  signaling was similar to wild type NK1 (Fig. 6). This underlines the crucial importance of the water hydrogen-bond network for fine-tuning the signaling of in this case the NK1 receptor through different signal transduction pathways (Fig. 7).

Interestingly, an interaction between AspII:10 (2.50) and AsnVII:16 (7.49) of the NPxxY motif in TM-VII was early on proposed in several receptors based on observations that paired swap of these two residues could restore receptor signaling, compared to the detrimental effects of each of the single mutations (50,63-65). Furthermore, rearrangements in this region during activation have also been shown for rhodopsin using radiolytic protein footprinting (66).

#### ***The water-gating residues of the hydrogen-bond network are essential for signaling in general***

Three residues appeared to be essential for all three signaling pathways  $G_q$ ,  $G_s$  and  $\beta$ -arrestin mobilization: the two water-gating micro-switch

residues, TrpVI:13 (6.48) and TyrVII:20 (7.53) and the totally conserved AsnI:18 (1.50) (Fig. 7). Originally we demonstrated by molecular dynamics simulations based on the high resolution structures of rhodopsin and B2AR that most of the water molecules of the network are highly mobile and that the entry and exit of these waters in and out of the network is gated by micro-switch residues, *i.e.* towards the ligand-binding pocket by TrpVI:13 and towards the intracellular cytosol by the rotary micro-switch TyrVII:20 (see central vignette in Figs 3-5) (5). Structures of active receptor conformations subsequently demonstrated that the ‘water volume’ of the hydrogen-bond network changes considerably in the transition between inactive and active conformations in which most of the water molecules are ‘squeezed’ out (16,27). Thus, the movement of water molecules in and out of the network and the gating of these must be essential for receptor function (5). Accordingly, in the present study of the NK1 receptor we find that both of the ‘water gating’ residues, TrpVI:13 and TyrVII:20 are essential for all three signaling pathways tested, just as we found they were essential for the Gs signaling in the B2AR (5). TrpVI:13 has been extensively studied and determined to be essential for receptor activation in multiple 7TM receptors (46). The rotameric micro-switch, TyrVII:20 in its inward rotameric form stabilizes the outward tilt of TM-VI (2), which opens a pocket between the helices allowing for G protein binding (29,67-70). AsnI:18 (1.50), which in the inactive receptor conformation makes a helix kink-stabilizing hydrogen-bond to the backbone carbonyl of the

residue in position VII:13 (7.46) exposed by the highly conserved ProVII:17 (7.50) of the NPxxY motif, is the only residue which is totally conserved throughout the entire, large rhodopsin-like family A of 7TM receptors (42). In the NK1 receptor the AsnI:18 (1.50) to Ala mutant abolished all receptor signaling. The extraordinary conservation of this residue in 7TM receptors would suggest that it is essential in receptor signaling in general. However, in the B2AR we found that the corresponding AsnI:18 to Ala substitution surprisingly had no effect on the agonist induced Gs signaling and in fact increased the constitutive activity (5).

**In conclusion** – Based on the X-ray structures, molecular dynamics simulations and mutational analysis we have previously proposed that the extended water hydrogen-bond network between TM-I, -II, -III, -VI and -VII constitutes an allosteric interface essential for stabilizing different active and inactive helical constellations during receptor activation (5). Here, we confirm that the water-gating micro-switch residues TrpVI:13 (6.48) of the CWxP motif and TyrVII:20 (7.53) of the NPxxY motif are essential for all signaling also in the NK1 receptor. Importantly, we identify the interaction between the unique Glu in position II:10 (2.50), SerIII:15 (3.39) and AsnVII:16 (7.49) of the NPxxY motif in TM-VII as a key point for determining Gs versus Gq signaling as well as  $\beta$ -arrestin mobilization. Specifically the interface between TM-II, -III and -VII appears to be particularly important for Gs signaling which could potentially be used in future drug discovery efforts. For example, it may be possible to generate agonists with an appropriate



signaling bias ensuring proper balance in efficacy through the Gs and the Gq pathways as recently described for the long chain fatty acid receptor GPR40 to obtain appropriate in vivo incretin releasing efficacy (71).

#### **Acknowledgement**

The Novo Nordisk Foundation Center for Basic Metabolic Research is based on an unconditional grant from the Novo Nordisk Foundation to the Faculty of Health Sciences at University of Copenhagen. LVH was recipient of a PhD scholarship from the Faculty of Health Sciences at University of Copenhagen. NDH was supported by funding from the Medical Research Council U.K. (Grant G0700049).

#### **Conflict of interest**

The authors declare that they have no conflicts of interest with the contents of this article.

#### **Author contributions**

LVH, TMF and TWS conceived the study and wrote the manuscript. LVH, JM and NDH performed and analyzed the experiments. All comparative homology modelling was conducted and analyzed by TMF. All authors

reviewed the results and approved the final version of the manuscript.

## Reference List

1. Rosenbaum, D. M., Rasmussen, S. G., and Kobilka, B. K. (2009) The structure and function of G-protein-coupled receptors. *Nature* **459**, 356-363
2. Nygaard, R., Frimurer, T. M., Holst, B., Rosenkilde, M. M., and Schwartz, T. W. (2009) Ligand binding and micro-switches in 7TM receptor structures. *Trends Pharmacol. Sci.* **30**, 249-259
3. Katritch, V., Cherezov, V., and Stevens, R. C. (2013) Structure-function of the G protein-coupled receptor superfamily. *Annu. Rev. Pharmacol. Toxicol.* **53**, 531-556
4. Wisler, J. W., Xiao, K., Thomsen, A. R., and Lefkowitz, R. J. (2014) Recent developments in biased agonism. *Curr. Opin. Cell Biol.* **27**, 18-24
5. Nygaard, R., Valentin-Hansen, L., Mokrosinski, J., Frimurer, T. M., and Schwartz, T. W. (2010) Conserved water-mediated hydrogen bond network between TM-I, -II, -VI, and -VII in 7TM receptor activation. *J. Biol. Chem.* **285**, 19625-19636
6. Stevens, R. C., Cherezov, V., Katritch, V., Abagyan, R., Kuhn, P., Rosen, H., and Wuthrich, K. (2013) The GPCR Network: a large-scale collaboration to determine human GPCR structure and function. *Nat. Rev. Drug Discov.* **12**, 25-34
7. Srivastava, A., Yano, J., Hirozane, Y., Kefala, G., Gruswitz, F., Snell, G., Lane, W., Ivetac, A., Aertgeerts, K., Nguyen, J., Jennings, A., and Okada, K. (2014) High-resolution structure of the human GPR40 receptor bound to allosteric agonist TAK-875. *Nature*
8. Zhang, K., Zhang, J., Gao, Z. G., Zhang, D., Zhu, L., Han, G. W., Moss, S. M., Paoletta, S., Kiselev, E., Lu, W., Fenalti, G., Zhang, W., Muller, C. E., Yang, H., Jiang, H., Cherezov, V., Katritch, V., Jacobson, K. A., Stevens, R. C., Wu, B., and Zhao, Q. (2014) Structure of the human P2Y12 receptor in complex with an antithrombotic drug. *Nature* **509**, 115-118
9. Tan, Q., Zhu, Y., Li, J., Chen, Z., Han, G. W., Kufareva, I., Li, T., Ma, L., Fenalti, G., Li, J., Zhang, W., Xie, X., Yang, H., Jiang, H., Cherezov, V., Liu, H., Stevens, R. C., Zhao, Q., and Wu, B. (2013) Structure of the CCR5 chemokine receptor-HIV entry inhibitor maraviroc complex. *Science* **341**, 1387-1390

10. Cherezov, V., Rosenbaum, D. M., Hanson, M. A., Rasmussen, S. G., Thian, F. S., Kobilka, T. S., Choi, H. J., Kuhn, P., Weis, W. I., Kobilka, B. K., and Stevens, R. C. (2007) High-resolution crystal structure of an engineered human beta2-adrenergic G protein-coupled receptor. *Science* **318**, 1258-1265
11. Chien, E. Y., Liu, W., Zhao, Q., Katritch, V., Han, G. W., Hanson, M. A., Shi, L., Newman, A. H., Javitch, J. A., Cherezov, V., and Stevens, R. C. (2010) Structure of the human dopamine D3 receptor in complex with a D2/D3 selective antagonist. *Science* **330**, 1091-1095
12. Granier, S., Manglik, A., Kruse, A. C., Kobilka, T. S., Thian, F. S., Weis, W. I., and Kobilka, B. K. (2012) Structure of the delta-opioid receptor bound to naltrindole. *Nature* **485**, 400-404
13. Haga, K., Kruse, A. C., Asada, H., Yurugi-Kobayashi, T., Shiroishi, M., Zhang, C., Weis, W. I., Okada, T., Kobilka, B. K., Haga, T., and Kobayashi, T. (2012) Structure of the human M2 muscarinic acetylcholine receptor bound to an antagonist. *Nature* **482**, 547-551
14. Hanson, M. A., Roth, C. B., Jo, E., Griffith, M. T., Scott, F. L., Reinhart, G., Desale, H., Clemons, B., Cahalan, S. M., Schuerer, S. C., Sanna, M. G., Han, G. W., Kuhn, P., Rosen, H., and Stevens, R. C. (2012) Crystal structure of a lipid G protein-coupled receptor. *Science* **335**, 851-855
15. Kruse, A. C., Hu, J., Pan, A. C., Arlow, D. H., Rosenbaum, D. M., Rosemond, E., Green, H. F., Liu, T., Chae, P. S., Dror, R. O., Shaw, D. E., Weis, W. I., Wess, J., and Kobilka, B. K. (2012) Structure and dynamics of the M3 muscarinic acetylcholine receptor. *Nature* **482**, 552-556
16. Liu, W., Chun, E., Thompson, A. A., Chubukov, P., Xu, F., Katritch, V., Han, G. W., Roth, C. B., Heitman, L. H., Ijzerman, A. P., Cherezov, V., and Stevens, R. C. (2012) Structural basis for allosteric regulation of GPCRs by sodium ions. *Science* **337**, 232-236
17. Manglik, A., Kruse, A. C., Kobilka, T. S., Thian, F. S., Mathiesen, J. M., Sunahara, R. K., Pardo, L., Weis, W. I., Kobilka, B. K., and Granier, S. (2012) Crystal structure of the micro-opioid receptor bound to a morphinan antagonist. *Nature* **485**, 321-326
18. Ruprecht, J. J., Mielke, T., Vogel, R., Villa, C., and Schertler, G. F. (2004) Electron crystallography reveals the structure of metarhodopsin I. *EMBO J.* **23**, 3609-3620
19. Shimamura, T., Shiroishi, M., Weyand, S., Tsujimoto, H., Winter, G., Katritch, V., Abagyan, R., Cherezov, V., Liu, W., Han, G. W., Kobayashi, T., Stevens, R. C., and Iwata, S. (2011) Structure of the human histamine H1 receptor complex with doxepin. *Nature* **475**, 65-70

20. Thompson, A. A., Liu, W., Chun, E., Katritch, V., Wu, H., Vardy, E., Huang, X. P., Trapella, C., Guerrini, R., Calo, G., Roth, B. L., Cherezov, V., and Stevens, R. C. (2012) Structure of the nociceptin/orphanin FQ receptor in complex with a peptide mimetic. *Nature* **485**, 395-399
21. Wacker, D., Wang, C., Katritch, V., Han, G. W., Huang, X. P., Vardy, E., McCorvy, J. D., Jiang, Y., Chu, M., Siu, F. Y., Liu, W., Xu, H. E., Cherezov, V., Roth, B. L., and Stevens, R. C. (2013) Structural features for functional selectivity at serotonin receptors. *Science* **340**, 615-619
22. Wang, C., Jiang, Y., Ma, J., Wu, H., Wacker, D., Katritch, V., Han, G. W., Liu, W., Huang, X. P., Vardy, E., McCorvy, J. D., Gao, X., Zhou, X. E., Melcher, K., Zhang, C., Bai, F., Yang, H., Yang, L., Jiang, H., Roth, B. L., Cherezov, V., Stevens, R. C., and Xu, H. E. (2013) Structural basis for molecular recognition at serotonin receptors. *Science* **340**, 610-614
23. Warne, T., Serrano-Vega, M. J., Baker, J. G., Moukhametzianov, R., Edwards, P. C., Henderson, R., Leslie, A. G., Tate, C. G., and Schertler, G. F. (2008) Structure of a beta1-adrenergic G-protein-coupled receptor. *Nature* **454**, 486-491
24. Wu, B., Chien, E. Y., Mol, C. D., Fenalti, G., Liu, W., Katritch, V., Abagyan, R., Brooun, A., Wells, P., Bi, F. C., Hamel, D. J., Kuhn, P., Handel, T. M., Cherezov, V., and Stevens, R. C. (2010) Structures of the CXCR4 chemokine GPCR with small-molecule and cyclic peptide antagonists. *Science* **330**, 1066-1071
25. Wu, H., Wacker, D., Mileni, M., Katritch, V., Han, G. W., Vardy, E., Liu, W., Thompson, A. A., Huang, X. P., Carroll, F. I., Mascarella, S. W., Westkaemper, R. B., Mosier, P. D., Roth, B. L., Cherezov, V., and Stevens, R. C. (2012) Structure of the human kappa-opioid receptor in complex with JDTic. *Nature* **485**, 327-332
26. Zhang, C., Srinivasan, Y., Arlow, D. H., Fung, J. J., Palmer, D., Zheng, Y., Green, H. F., Pandey, A., Dror, R. O., Shaw, D. E., Weis, W. I., Coughlin, S. R., and Kobilka, B. K. (2012) High-resolution crystal structure of human protease-activated receptor 1. *Nature* **492**, 387-392
27. Fenalti, G., Giguere, P. M., Katritch, V., Huang, X. P., Thompson, A. A., Cherezov, V., Roth, B. L., and Stevens, R. C. (2014) Molecular control of delta-opioid receptor signalling. *Nature*
28. Gutierrez-de-Teran, H., Massink, A., Rodriguez, D., Liu, W., Han, G. W., Joseph, J. S., Katritch, I., Heitman, L. H., Xia, L., Ijzerman, A. P., Cherezov, V., Katritch, V., and Stevens, R. C. (2013) The Role of a Sodium Ion Binding Site in the Allosteric Modulation of the A2A Adenosine G Protein-Coupled Receptor. *Structure*. **21**, 2175-2185

29. Rasmussen, S. G., DeVree, B. T., Zou, Y., Kruse, A. C., Chung, K. Y., Kobilka, T. S., Thian, F. S., Chae, P. S., Pardon, E., Calinski, D., Mathiesen, J. M., Shah, S. T., Lyons, J. A., Caffrey, M., Gellman, S. H., Steyaert, J., Skiniotis, G., Weis, W. I., Sunahara, R. K., and Kobilka, B. K. (2011) Crystal structure of the beta2 adrenergic receptor-Gs protein complex. *Nature* **477**, 549-555
30. Xu, F., Wu, H., Katritch, V., Han, G. W., Jacobson, K. A., Gao, Z. G., Cherezov, V., and Stevens, R. C. (2011) Structure of an agonist-bound human A2A adenosine receptor. *Science* **332**, 322-327
31. Costa, T., Lang, J., Gless, C., and Herz, A. (1990) Spontaneous association between opioid receptors and GTP-binding regulatory proteins in native membranes: specific regulation by antagonists and sodium ions. *Mol. Pharmacol.* **37**, 383-394
32. Gao, Z. G. and Ijzerman, A. P. (2000) Allosteric modulation of A(2A) adenosine receptors by amiloride analogues and sodium ions. *Biochem. Pharmacol.* **60**, 669-676
33. Horstman, D. A., Brandon, S., Wilson, A. L., Guyer, C. A., Cragoe, E. J., Jr., and Limbird, L. E. (1990) An aspartate conserved among G-protein receptors confers allosteric regulation of alpha 2-adrenergic receptors by sodium. *J. Biol. Chem.* **265**, 21590-21595
34. Selent, J., Sanz, F., Pastor, M., and De, F. G. (2010) Induced effects of sodium ions on dopaminergic G-protein coupled receptors. *PLoS. Comput. Biol.* **6**,
35. Wilson, M. H., Highfield, H. A., and Limbird, L. E. (2001) The role of a conserved inter-transmembrane domain interface in regulating alpha(2a)-adrenergic receptor conformational stability and cell-surface turnover. *Mol. Pharmacol.* **59**, 929-938
36. Schwartz, T. W. and Holst, B. (2007) Allosteric enhancers, allosteric agonists and ago-allosteric modulators: where do they bind and how do they act? *Trends Pharmacol. Sci.* **28**, 366-373
37. Katritch, V., Fenalti, G., Abola, E. E., Roth, B. L., Cherezov, V., and Stevens, R. C. (2014) Allosteric sodium in class A GPCR signaling. *Trends Biochem. Sci.* **39**, 233-244
38. Holst, B., Hastrup, H., Raffetseder, U., Martini, L., and Schwartz, T. W. (2001) Two active molecular phenotypes of the tachykinin NK1 receptor revealed by G-protein fusions and mutagenesis. *J. Biol. Chem.* **276**, 19793-19799



39. Martini, L., Hastrup, H., Holst, B., Fraile-Ramos, A., Marsh, M., and Schwartz, T. W. (2002) NK1 receptor fused to beta-arrestin displays a single-component, high-affinity molecular phenotype. *Mol. Pharmacol.* **62**, 30-37
40. Quartara, L. and Maggi, C. A. (1997) The tachykinin NK1 receptor. Part I: ligands and mechanisms of cellular activation. *Neuropeptides* **31**, 537-563
41. Schwartz, T. W., Frimurer, T. M., Holst, B., Rosenkilde, M. M., and Elling, C. E. (2006) Molecular mechanism of 7TM receptor activation--a global toggle switch model. *Annu. Rev. Pharmacol. Toxicol.* **46**, 481-519
42. Mirzadegan, T., Benko, G., Filipek, S., and Palczewski, K. (2003) Sequence analyses of G-protein-coupled receptors: similarities to rhodopsin. *Biochemistry* **42**, 2759-2767
43. Gether, U., Johansen, T. E., Snider, R. M., Lowe, J. A., III, Nakanishi, S., and Schwartz, T. W. (1993) Different binding epitopes on the NK1 receptor for substance P and non-peptide antagonist. *Nature* **362**, 345-348
44. Gether, U., Yokota, Y., Emonds-Alt, X., Breliere, J. C., Lowe, J. A., III, Snider, R. M., Nakanishi, S., and Schwartz, T. W. (1993) Two nonpeptide tachykinin antagonists act through epitopes on corresponding segments of the NK1 and NK2 receptors. *Proc. Natl. Acad. Sci. U. S. A* **90**, 6194-6198
45. Holst, B., Zoffmann, S., Elling, C. E., Hjorth, S. A., and Schwartz, T. W. (1998) Steric hindrance mutagenesis versus alanine scan in mapping of ligand binding sites in the tachykinin NK1 receptor. *Mol. Pharmacol.* **53**, 166-175
46. Holst, B., Nygaard, R., Valentin-Hansen, L., Bach, A., Engelstoft, M. S., Petersen, P. S., Frimurer, T. M., and Schwartz, T. W. (2010) A conserved aromatic lock for the tryptophan rotameric switch in TM-VI of seven-transmembrane receptors. *J. Biol. Chem.* **285**, 3973-3985
47. Nielsen, S. M., Elling, C. E., and Schwartz, T. W. (1998) Split-receptors in the tachykinin neurokinin-1 system--mutational analysis of intracellular loop 3. *Eur. J. Biochem.* **251**, 217-226
48. Miller-Gallacher, J. L., Nehme, R., Warne, T., Edwards, P. C., Schertler, G. F., Leslie, A. G., and Tate, C. G. (2014) The 2.1 Å resolution structure of cyanopindolol-bound beta1-adrenoceptor identifies an intramembrane Na<sup>+</sup> ion that stabilises the ligand-free receptor. *PLoS One.* **9**, e92727

49. Tan, Q., Zhu, Y., Li, J., Chen, Z., Han, G. W., Kufareva, I., Li, T., Ma, L., Fenalti, G., Li, J., Zhang, W., Xie, X., Yang, H., Jiang, H., Cherezov, V., Liu, H., Stevens, R. C., Zhao, Q., and Wu, B. (2013) Structure of the CCR5 chemokine receptor-HIV entry inhibitor maraviroc complex. *Science* **341**, 1387-1390
50. Zhou, W., Flanagan, C., Ballesteros, J. A., Konvicka, K., Davidson, J. S., Weinstein, H., Millar, R. P., and Sealfon, S. C. (1994) A reciprocal mutation supports helix 2 and helix 7 proximity in the gonadotropin-releasing hormone receptor. *Mol. Pharmacol.* **45**, 165-170
51. Jaakola, V. P., Griffith, M. T., Hanson, M. A., Cherezov, V., Chien, E. Y., Lane, J. R., Ijzerman, A. P., and Stevens, R. C. (2008) The 2.6 angstrom crystal structure of a human A2A adenosine receptor bound to an antagonist. *Science* **322**, 1211-1217
52. Sivertsen, B., Lang, M., Frimurer, T. M., Holliday, N. D., Bach, A., Els, S., Engelstoft, M. S., Petersen, P. S., Madsen, A. N., Schwartz, T. W., Beck-Sickinger, A. G., and Holst, B. (2011) Unique interaction pattern for a functionally biased ghrelin receptor agonist. *J. Biol. Chem.* **286**, 20845-20860
53. Jin, L. Q., Wang, H. Y., and Friedman, E. (2001) Stimulated D(1) dopamine receptors couple to multiple Galpha proteins in different brain regions. *J. Neurochem.* **78**, 981-990
54. Kilts, J. D., Gerhardt, M. A., Richardson, M. D., Sreeram, G., Mackensen, G. B., Grocott, H. P., White, W. D., Davis, R. D., Newman, M. F., Reves, J. G., Schwinn, D. A., and Kwatra, M. M. (2000) Beta(2)-adrenergic and several other G protein-coupled receptors in human atrial membranes activate both G(s) and G(i). *Circ. Res.* **87**, 705-709
55. Laugwitz, K. L., Allgeier, A., Offermanns, S., Spicher, K., Van, S. J., Dumont, J. E., and Schultz, G. (1996) The human thyrotropin receptor: a heptahelical receptor capable of stimulating members of all four G protein families. *Proc. Natl. Acad. Sci. U. S. A* **93**, 116-120
56. Govaerts, C., Lefort, A., Costagliola, S., Wodak, S. J., Ballesteros, J. A., Van, S. J., Pardo, L., and Vassart, G. (2001) A conserved Asn in transmembrane helix 7 is an on/off switch in the activation of the thyrotropin receptor. *J. Biol. Chem.* **276**, 22991-22999
57. Gales, C., Kowalski-Chauvel, A., Dufour, M. N., Seva, C., Moroder, L., Pradayrol, L., Vaysse, N., Fourmy, D., and Silvente-Poirot, S. (2000) Mutation of Asn-391 within the conserved NPXXY motif of the cholecystokinin B receptor abolishes Gq protein activation without affecting its association with the receptor. *J. Biol. Chem.* **275**, 17321-17327

58. Webb, D. R., Handel, T. M., Kretz-Rommel, A., and Stevens, R. C. (2013) Opportunities for functional selectivity in GPCR antibodies. *Biochem. Pharmacol.* **85**, 147-152
59. Luttrell, L. M. (2014) Minireview: More than just a hammer: ligand "bias" and pharmaceutical discovery. *Mol. Endocrinol.* **28**, 281-294
60. Shukla, A. K., Violin, J. D., Whalen, E. J., Gesty-Palmer, D., Shenoy, S. K., and Lefkowitz, R. J. (2008) Distinct conformational changes in beta-arrestin report biased agonism at seven-transmembrane receptors. *Proc. Natl. Acad. Sci. U. S. A* **105**, 9988-9993
61. Wei, H., Ahn, S., Shenoy, S. K., Karnik, S. S., Hunyady, L., Luttrell, L. M., and Lefkowitz, R. J. (2003) Independent beta-arrestin 2 and G protein-mediated pathways for angiotensin II activation of extracellular signal-regulated kinases 1 and 2. *Proc. Natl. Acad. Sci. U. S. A* **100**, 10782-10787
62. Steen, A., Thiele, S., Guo, D., Hansen, L. S., Frimurer, T. M., and Rosenkilde, M. M. (2013) Biased and constitutive signaling in the CC-chemokine receptor CCR5 by manipulating the interface between transmembrane helices 6 and 7. *J. Biol. Chem.* **288**, 12511-12521
63. Urizar, E., Claeysen, S., Deupi, X., Govaerts, C., Costagliola, S., Vassart, G., and Pardo, L. (2005) An activation switch in the rhodopsin family of G protein-coupled receptors: the thyrotropin receptor. *J. Biol. Chem.* **280**, 17135-17141
64. Sealfon, S. C., Chi, L., Ebersole, B. J., Rodic, V., Zhang, D., Ballesteros, J. A., and Weinstein, H. (1995) Related contribution of specific helix 2 and 7 residues to conformational activation of the serotonin 5-HT<sub>2A</sub> receptor. *J. Biol. Chem.* **270**, 16683-16688
65. Nikiforovich, G. V., Zhang, M., Yang, Q., Jagadeesh, G., Chen, H. C., Hunyady, L., Marshall, G. R., and Catt, K. J. (2006) Interactions between conserved residues in transmembrane helices 2 and 7 during angiotensin AT<sub>1</sub> receptor activation. *Chem. Biol. Drug Des* **68**, 239-249
66. Angel, T. E., Gupta, S., Jastrzebska, B., Palczewski, K., and Chance, M. R. (2009) Structural waters define a functional channel mediating activation of the GPCR, rhodopsin. *Proc. Natl. Acad. Sci. U. S. A* **106**, 14367-14372
67. Choe, H. W., Kim, Y. J., Park, J. H., Morizumi, T., Pai, E. F., Krauss, N., Hofmann, K. P., Scheerer, P., and Ernst, O. P. (2011) Crystal structure of metarhodopsin II. *Nature* **471**, 651-655

68. Park, J. H., Scheerer, P., Hofmann, K. P., Choe, H. W., and Ernst, O. P. (2008) Crystal structure of the ligand-free G-protein-coupled receptor opsin. *Nature* **454**, 183-187
69. Rasmussen, S. G., Choi, H. J., Fung, J. J., Pardon, E., Casarosa, P., Chae, P. S., DeVree, B. T., Rosenbaum, D. M., Thian, F. S., Kobilka, T. S., Schnapp, A., Konetzki, I., Sunahara, R. K., Gellman, S. H., Pautsch, A., Steyaert, J., Weis, W. I., and Kobilka, B. K. (2011) Structure of a nanobody-stabilized active state of the beta(2) adrenoceptor. *Nature* **469**, 175-180
70. Scheerer, P., Park, J. H., Hildebrand, P. W., Kim, Y. J., Krauss, N., Choe, H. W., Hofmann, K. P., and Ernst, O. P. (2008) Crystal structure of opsin in its G-protein-interacting conformation. *Nature* **455**, 497-502
71. Hauge, M., Vestmar, M. A., Husted, A. S., Ekberg, J. P., Wright, M. J., Di, S. J., Weinglass, A. B., Engelstoft, M. S., Madsen, A. N., Luckmann, M., Miller, M. W., Trujillo, M. E., Frimurer, T. M., Holst, B., Howard, A. D., and Schwartz, T. W. (2015) GPR40 (FFAR1) - Combined Gs and Gq signaling in vitro is associated with robust incretin secretagogue action ex vivo and in vivo. *Mol. Metab* **4**, 3-14

## Footnotes

1 The abbreviations used are: TM, transmembrane; 7TM, 7-transmembrane; B2AR,  $\beta$ 2-adrenergic receptor; A<sub>2A</sub>AR, adenosine A<sub>2A</sub> receptor; NTSR1, neurotensin-1 receptor; NK1, neurokinin-1; ELISA, enzyme-linked immunosorbent assay.

2 The Schwartz/Baldwin generic numbering system for 7TM receptors, which is based on the actual location of the residues in each trans-membrane helix, is used throughout the article (41)

## Figure legends

**Figure 1. Structural conservation of the polar interface between TM-I, -II, -III and -VII.** *Panel A*-Structural distribution of conserved polar residues between the intracellular half of TM-I, -II, -III, and -VII of 18 unique inactive GPCR structures. The residues AsnI:18, (1.50), AspII:10 (2.50), SerIII:15 (3.39), SerVII:12 (7.45), ThrVII:13 (7.46) and AsnVII:16 (7.49) of the conserved polar interface restricted by the functional important and conserved TrpVI:13 (6.48) and TyrVII:20 (7.53) in the antagonist bound structures of A<sub>2A</sub>AR (PDBID:4E1Y solved at 1.8 Å resolution) (blue), B2AR (PDBID: 2RH1) (yellow) are shown in sticks. The corresponding residues in the other inactive structures are shown by grey lines. *Panel B*-Close-up view of the polar interface comprising a sodium ion (purple sphere) and water molecules (red spheres). Co-localized water molecules in the A<sub>2A</sub>AR and the B2AR structure are shown as yellow spheres. The salt-bridge between sodium and AspII:10

(2.50) and water mediated hydrogen bond interactions are shown as grey dotted lines. *Panel C*- Close-up view of the polar pocket in the active-like agonist bound A<sub>2A</sub>AR/UK432,097 structure (PDBID: 3QAK) (blue) and the active agonist bound B<sub>2</sub>AR structure in complex with G<sub>s</sub> (PDBID: 3SN6). *Panel D*-Polar pocket alignment of the distinct inactive experimental structures compared to the conforming sequence in the NK1 receptor, which have a Glutamic acid instead of the highly conserved AspII:10 (2.50). *Panel E-F*-Structural details of AspII:10 Glu substitution (green) in the inactive A<sub>2A</sub>AR structure (E, First rotamer conformation of AspII:10 Glu substitution, F, Second rotamer conformation of AspII:10 Glu substitution). Water molecules that make steric clashes with the substituted Glutamic acid are shown as big transparent spheres.

**Figure 2. NK1 receptor models** *Panel A*- Side and top close-up view of the conserved polar interface including AsnI:18 (1.50), GluII:10 (2.50), SerIII:15 (3.39), SerVII:12 (7.45), ThrVII:13 (7.46) and AsnVII:16 (7.49) in the inactive NK1 receptor model restricted by the functional important and conserved residues TrpVI:13 (6.48) and TyrVII:20 (7.53). Water molecules are shown as red spheres and hydrogen bonds in grey dotted lines. In contrast to highly conserved AspII:10, the longer GluII:10 side-chain in the NK1 model is predicted to make direct, rather than water mediated interactions with SerIII:15 and AsnVII:16. Dashed red arrows shows the conformational rearrangements of TM-II, -III and -VII (illustrated by light green and transparent circles) required to obtain an “active” NK1 receptor structure consistent with common conformational changes observed in distinct active structures. *Panel B*-Model of the conserved polar interface of the NK1 receptor in an “active” state, based on the agonist-bound A<sub>2A</sub>AR structure (PDBID: 3QAK).

**Figure 3. Functional consequence of Ala substitution on G<sub>q</sub> signaling of the conserved polar residues in the NK1 receptor** *Panel a*- Structure of the hydrogen bond network in the NK1 receptor model based on A<sub>2A</sub>AR (PDBID: 4EIY) as a template structure. Key side-chains are shown in sticks and water molecules as red spheres. *Panel b-h*- Agonist (SP)-induced IP<sub>3</sub> production in COS-7 cells transiently transfected with either wild-type NK1 (dotted lines) or mutant forms of ThrVII:13Ala (7.46) (b), GluII:10Ala (2.50) (c), AsnI:18Ala (1.50) (d), SerIII:15Ala (3.39) (e), SerVII:12Ala (7.45) (f), AsnVII:16Ala (7.49) (g), TrpVI:13Ala (6.48) (h) and TyrVII:20Ala (7.53) (i). Cell surface receptor expression measured by ELISA is shown in the inserted column diagrams in each panel.

**Figure 4. Functional consequence of Ala substitution on G<sub>s</sub> signaling of the conserved polar residues in the NK1 receptor** *Panel a*- Structure of the hydrogen bond network in the NK1 receptor model based on A<sub>2A</sub>AR (PDBID: 4EIY) as a template structure. Key side-chains are shown in sticks and water molecules as red spheres. *Panel b-h*- Agonist (SP)-induced cAMP production in COS-7 cells transiently transfected with either wild-type NK1 (dotted lines) or mutant forms of ThrVII:13Ala



(7.46) (b), GluII:10Ala (2.50) (c), AsnI:18Ala (1.50) (d), SerIII:15Ala (3.39) (e), SerVII:12Ala (7.45) (f), AsnVII:16Ala (7.49) (g), TrpVI:13Ala (6.48) (h) and TyrVII:20Ala (7.53) (i).

**Figure 5. Functional consequence of Ala substitution on  $\beta$ -Arrestin2 mobilization of the conserved polar residues in the NK1 receptor** *Panel a-* Structure of the hydrogen bond network in the NK1 receptor model based on A<sub>2A</sub>AR (PDBID: 4EIY) as a template structure. Key side-chains are shown in sticks and water molecules as red spheres. *Panel b-h-* Agonist (SP)-induced  $\beta$ -Arrestin2 mobilization in CHOK1 cells transiently transfected with either wild-type NK1 (dotted lines) or mutant forms of ThrVII:13Ala (7.46) (b), GluII:10Ala (2.50) (c), AsnI:18Ala (1.50) (d), SerIII:15Ala (3.39) (e), SerVII:12Ala (7.45) (f), AsnVII:16Ala (7.49) (g), TrpVI:13Ala (6.48) (h) and TyrVII:20Ala (7.53) (i).

**Figure 6. Functional consequence of Asp substitution of the GluII:10 (2.50) residue in the NK1 receptor** *Panel a-c-* Agonist (SP)-induced IP<sub>3</sub> (b), cAMP (c) or  $\beta$ -Arrestin2 (d) mobilization in COS-7 cells (IP<sub>3</sub> and cAMP) or CHOK1 cells ( $\beta$ -Arrestin2) transiently transfected with either wild-type NK1 (dotted lines) or mutant GluII:10Ala/Asp. Cell surface receptor expression measured by ELISA is shown in the inserted column diagram in the panel b.

**Figure 7. Residues of the water hydrogen-bond network of the NK1 receptor identified to be either essential for overall signal transduction or for the fine-tuning and bias of signaling through the three different signaling pathways: Gs, Gq and  $\beta$ -arrestin.** Three residues were by Ala-substitutions identified to be essential for all three signal transduction pathways: the water-gating TrpVI:13 (6.48) of the CWxP motif and the TyrVII:20 (7.53) of the NPxxY motif as well as the ultra-highly conserved, TM-VII kink-stabilizing AsnI:18 (1.50). Mutations of GluII:10 (2.50), which in the NK1 receptor uniquely replaces the otherwise highly conserved AspII:10, and the two residues, which according to the molecular models, makes direct hydrogen bond interactions with, SerIII:15 (3.39) and AsnVII:16 (7.49) creates receptor mutants with biased signaling though:  $\beta$ -arrestin only (GluII:10 to Ala), Gq only (GluII:10 to Asp), high constitutive Gs signaling (GluII:10 to Gln) and Gq plus  $\beta$ -arrestin but not Gs (AsnVII:16 to Ala). Ala-substitution of SerIII:15 selectively increases Gs signaling from zero to approx. 40% of E<sub>max</sub>.

## Tables

Construct	Expression level	IP <sub>3</sub>			cAMP			β-Arrestin2				
		<i>n</i>	<i>EC</i> <sub>50</sub> (nM)	<i>E</i> <sub>max</sub>	<i>n</i>	Constitutive Activity	<i>EC</i> <sub>50</sub> (nM)	<i>E</i> <sub>max</sub>	<i>n</i>	<i>EC</i> <sub>50</sub> (nM)	<i>E</i> <sub>max</sub>	<i>n</i>
NK1 WT	1	8	0.31±0.11	100	7	1.7±1.4	0.62±0.18	100	5	0.06±0.01	100	8
AsnI:18Ala (1.50)	0.81±0.07	3	-	-	3	9.3±6 <sup>***</sup>	-	-	4	-	-	4
GluII:10Ala (2.50)	0.56±0.05	4	-	-	3	10.8±6.7 <sup>**</sup>	-	-	4	0.29±0.03	20±3.4	6
GluII:10Gln	1.31±0.09	6	0.72±0.25	38.6±2.5	3	37.7±4.6 <sup>****</sup>	-	-	3	0.46±0.25	98.06±11.2	4
GluII:10Asp	1.49±0.09	4	0.35±0.12	85.2±6.3	4	12.0±6.6 <sup>ns</sup>	20.3±9.6	60.9±6.5	4	-	-	3
SerIII:15Ala (3.39)	0.85±0.05	3	0.42±0.11	113±5.3	6	37.4±6.1 <sup>****</sup>	1.29±0.35	156±17.7	6	0.07±0.02	157±21.0	10
TrpVI:13Ala (6.48)	0.73±0.05	3	-	-	3	-	0.95±0.43	14.0±4.9	4	-	-	4
SerVII:12Ala (7.45)	0.93±0.06	6	0.17±0.06	35.0±6.7	4	4.2±2.1 <sup>ns</sup>	-	-	5	0.03±0.007	45.8±4.5	6
ThrVII:13Ala (7.46)	0.84±0.07	4	0.58±0.13	133.4±9.4	4	13.9±4.4 <sup>*</sup>	0.23±0.08	85.5±4.8	4	0.08±0.04	95.2±5.7	6
AsnVII:16Ala (7.49)	0.90±0.06	5	0.35±0.07	76.7±8.1	5	-	-	-	4	0.23±0.07	74.8±8.9	6
TyrVII:20Ala (7.53)	0.78±0.07	3	-	-	3	-	-	-	5	0.05±0.02	9.3±2.0	4

**Table I**

**G<sub>q</sub>, G<sub>s</sub> and β-Arrestin signaling of the WT NK1 receptor and mutant forms with Ala substitution in positions Asn1:18 (1.50), GluII:10 (2.50), SerII:15Ala (3.39), TrpVI:13 (6.48), SerVII:12 (7.45), ThrVII:13 (7.46), AsnVII:16 (7.49) and TyrVII:20 (7.53) and Asp substitution in position GluII:10 (2.50).** The constructs were expressed in transiently transfected COS-7 cells (G<sub>q</sub> and G<sub>s</sub>) and CHOK1 cells (β-Arrestin). The *E<sub>max</sub>* values are expressed as percentage of the ligand-induced signaling for the WT NK1 receptor. Values are shown ± SE. Comparison between Constitutive activity of WT NK1 and the mutant receptors (P<0.05). (\* P=0,0108, \*\*P=0,0015, \*\*\*P =0,0009, \*\*\*\*P <0,0001). ns = not significant.

<i>Construct</i>	<i>n</i>	<i>K<sub>d</sub></i> (nM)				
		0mM NaCl	50mM NaCl	100mM NaCl	200mM NaCl	300mM NaCl
WT NK1	5	0.125±0.06	0.116±0.03	0.187±0.09	0.314±0.16	0.253±0.08
GluII:10A (2.50)	5	0.657±0.28	0.520±0.13	0.778±0.11	1.45±0.43	3.18±2.09
GluII:10D	5	0.114±0.04	0.128±0.02	0.204±0.06	0.290±0.07	1.20±0.54
SerIII:15A (3.39)	4	0.172±0.04	0.469±0.32	0.284±0.13	0.310±0.10	0.446±0.09

**Table II**

**Ligand binding properties of SP to WT NK1 receptor and substitutions in position GluII:10 (2.50) and SerIII:15 (3.39) in the NK1 receptor using [1125]SP as a radioligand.** The constructs were expressed in transiently transfected COS-7 cells. Values are shown ± S.E.

Construct	Expression level	<i>n</i>	<i>CA</i>	<i>EC</i> <sub>50</sub> (nM) (Ligand)	<i>E</i> <sub>max</sub>	<i>n</i>
<b>GHSR 1a WT</b>	1±0.02	3	43.4±2.06	0,36±0.27 (Ghrelin)	100	3
AspII:10Glu	0.60±0.06	3	-	-	-	3
<b>B2AR WT</b>	1±0.03	5	9.9±2.55	2.97±1.09 (Pindolol)	100	6
AspII:10Glu	0.68±0.06	5	2±1.92	5.68±2.90	16.6±5.35	5
<b>GPR119 WT</b>	1±0.09	5	43.6±3.43	2.22±0.34 (AR-231453)	100	5
AspII:10Glu	0.51±0.11	5	27.5±5.3	17.0±5.01	56±5.01	5

**Table III**

**G<sub>q</sub> or G<sub>s</sub> signaling of the WT GHSR, B2AR and GPR119 and the AspII:10Glu mutant variant of these receptors.** The constructs were expressed in transiently transfected COS-7 cells. The constitutive and ghrelin-induced G<sub>q</sub> signaling was determined for the Ghrelin receptor while signaling through the G<sub>s</sub> signaling pathway was determined for B2AR (pindolol) and GPR119 (AR-231453). The *E*<sub>max</sub> values are expressed as percentage of the ligand-induced signaling for the WT receptors. Values are shown ± SE.

## Figures

Figure 1

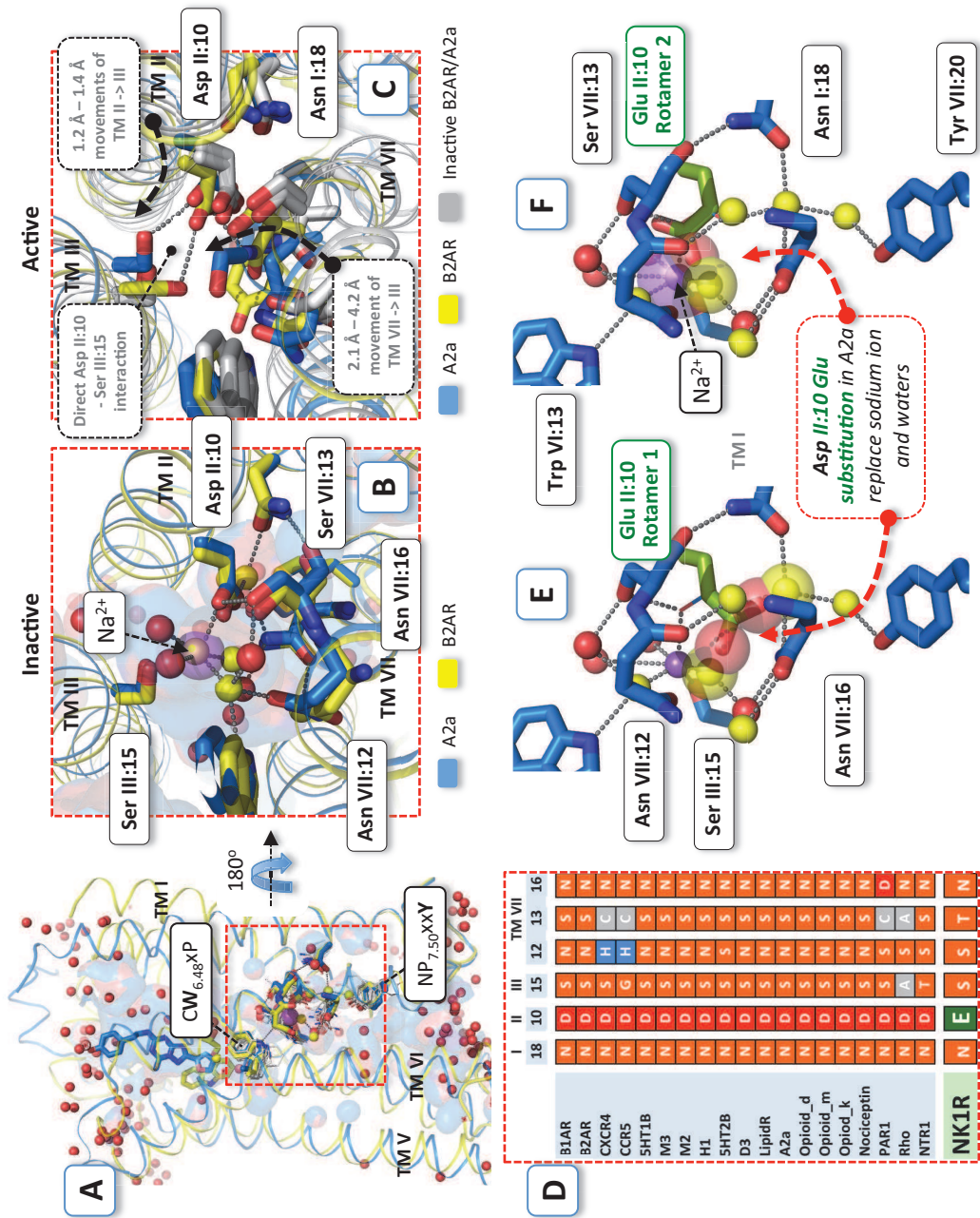


Figure 2

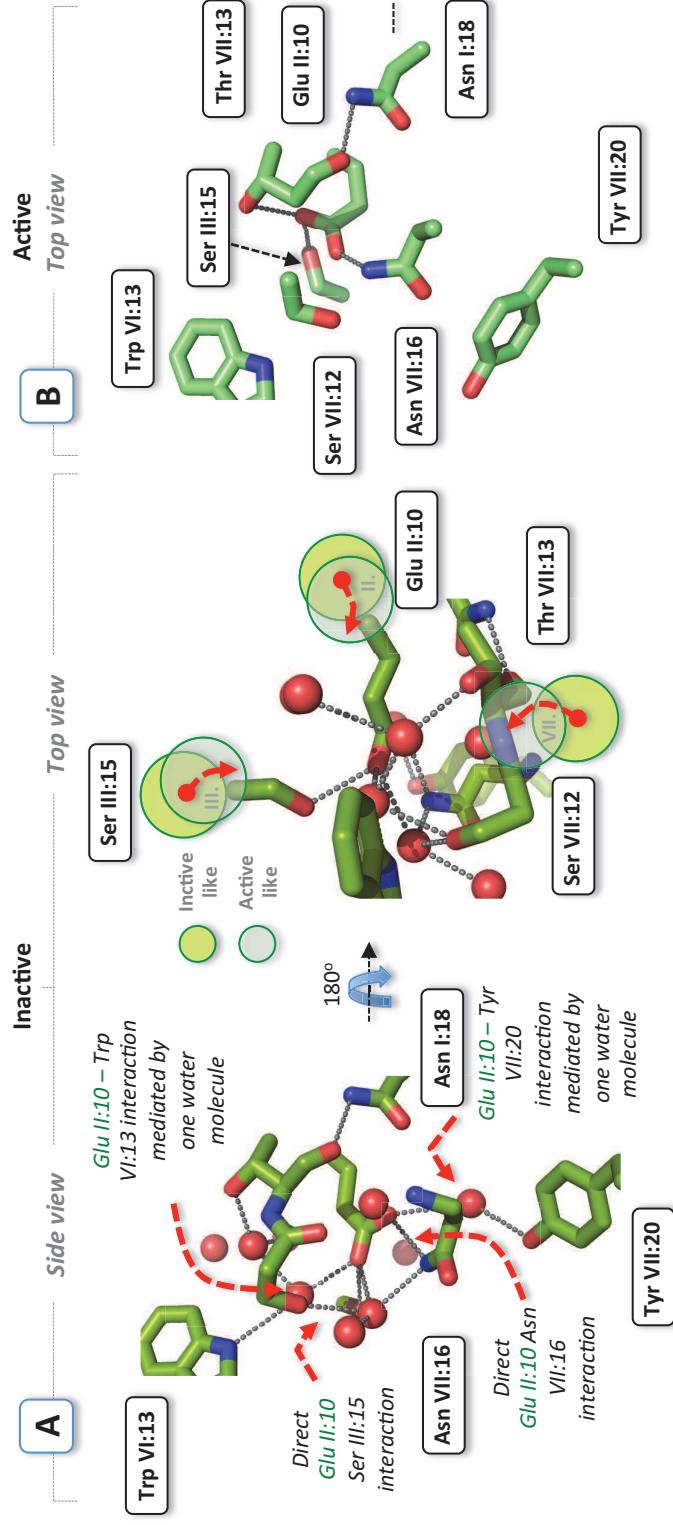




Figure 3

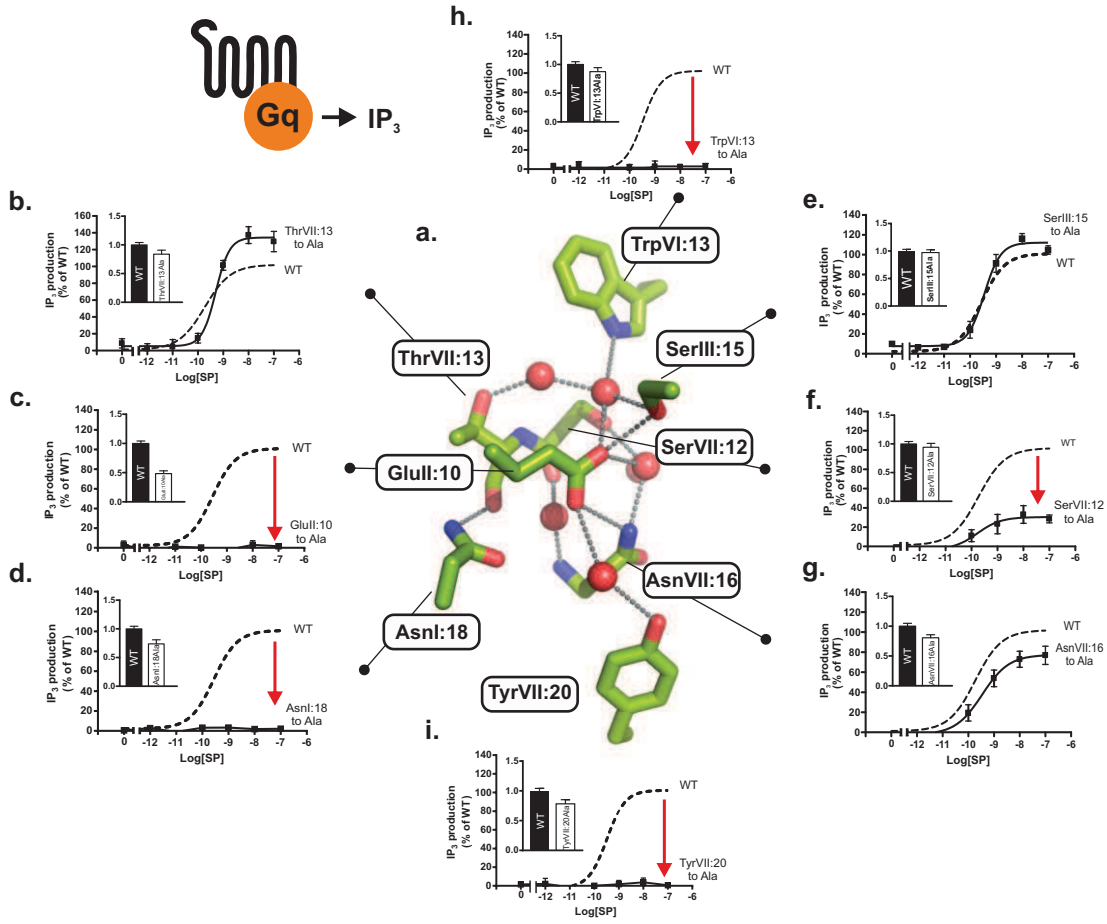


Figure 4

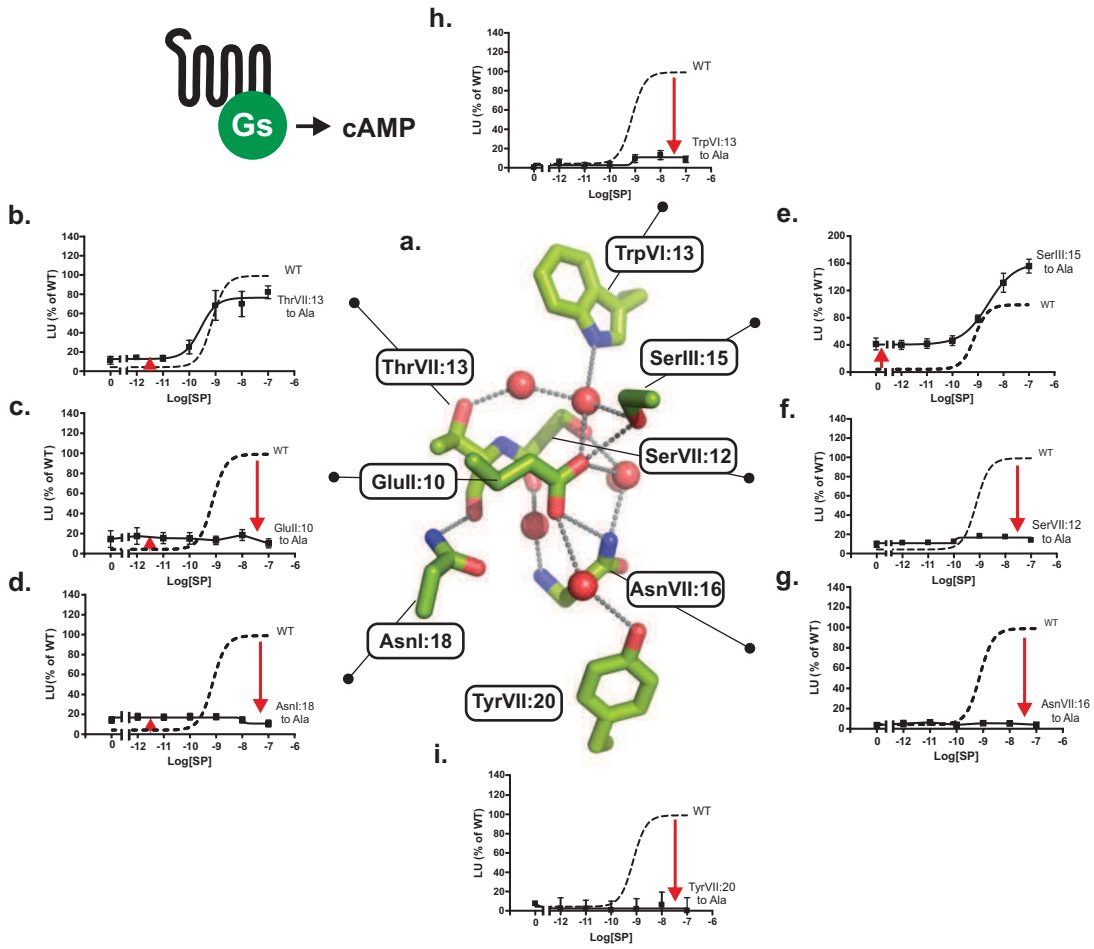


Figure 5

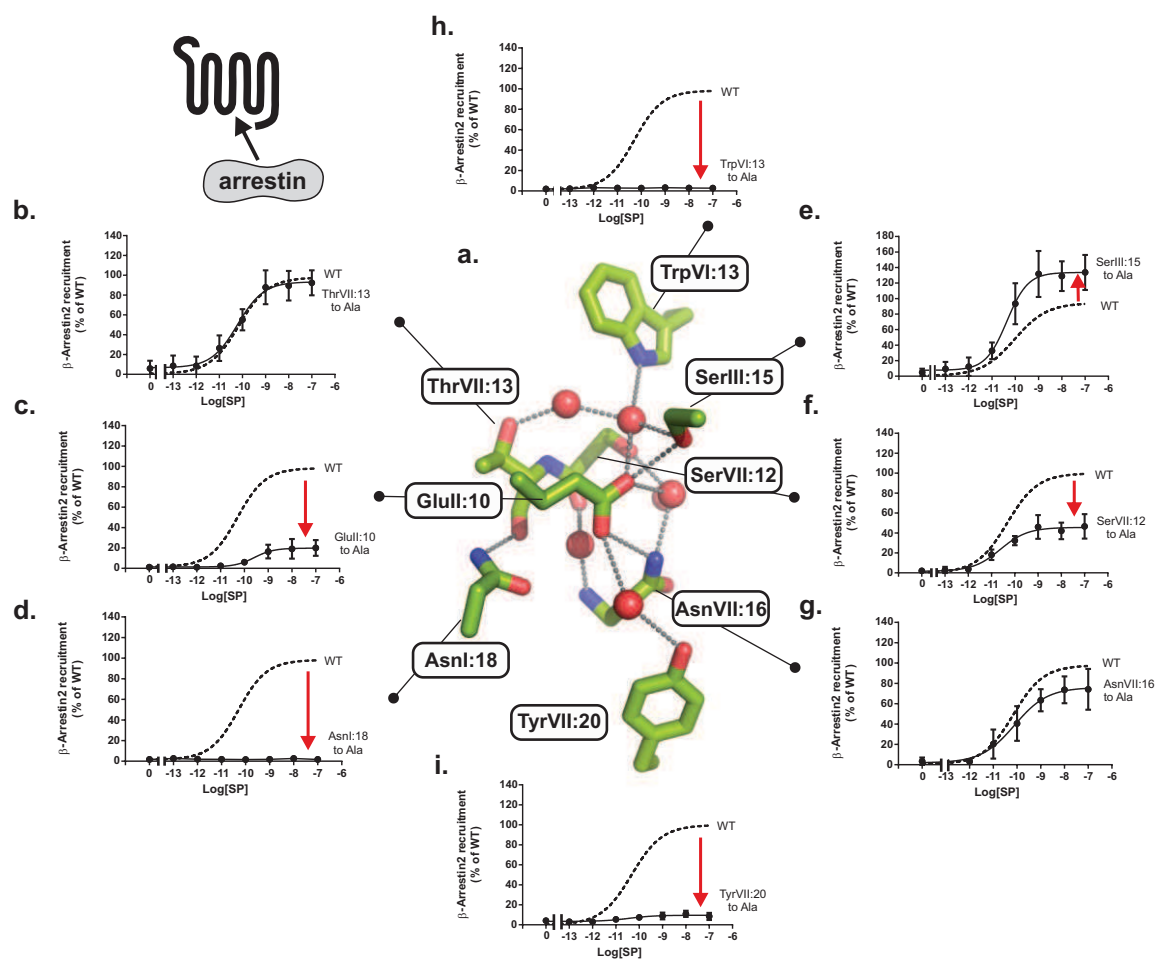


Figure 6

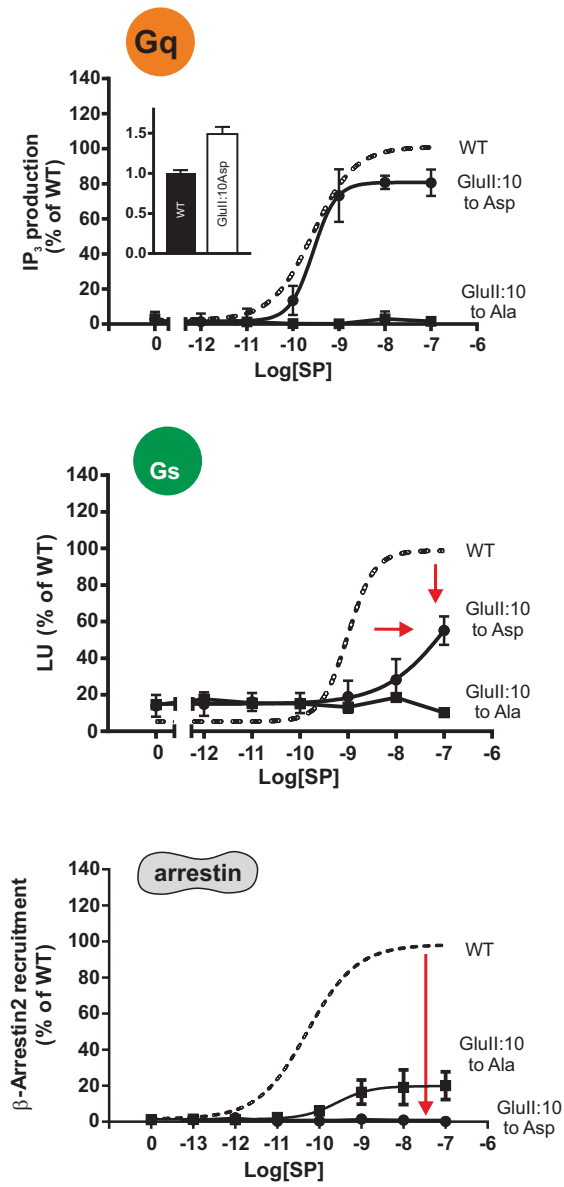
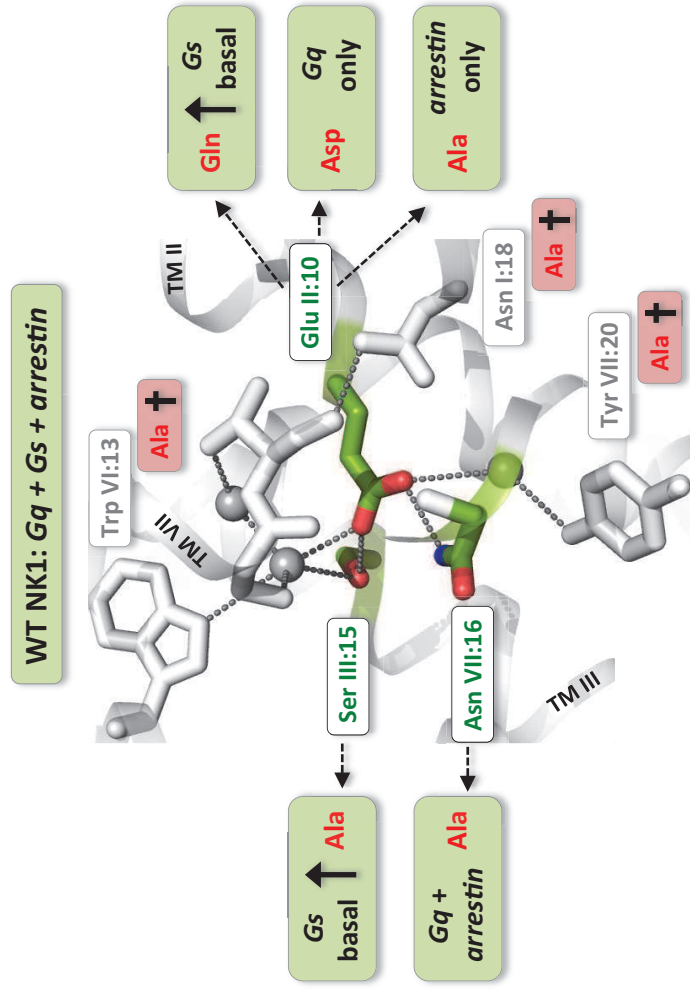


Figure 7



**Biased Gs versus Gq and  $\beta$ -arrestin signaling in the NK1 receptor determined by interactions in the water hydrogen-bond network**

Louise Valentin-Hansen, Thomas M. Frimurer, Jacek Mokrosinski, Nicholas D. Holliday and Thue W. Schwartz

*J. Biol. Chem.* published online August 12, 2015

---

Access the most updated version of this article at doi: [10.1074/jbc.M115.641944](https://doi.org/10.1074/jbc.M115.641944)

Alerts:

- [When this article is cited](#)
- [When a correction for this article is posted](#)

[Click here](#) to choose from all of JBC's e-mail alerts